Mem. S.A.It. Vol. 79, 756
© SAIt 2008

Memorie della

Reconstruction of Gaia marginals in crowded fields

F. Troisi[1], R. Buonanno[1,2], G. Iannicola[3], and L. Pulone[3]

[1] ASI-ASDC via Galileo Galilei, 00044 Frascati, Rome, Italy
e-mail: `licia.troisi@asdc.asi.it`
[2] University of Rome "Tor Vergata", Physics Department Via della Ricerca Scientifica 1, 00173 Rome, Italy
[3] INAF Astronomical Observatory of Rome, Via di Frascati, 00040 Monte Porzio Catone, Rome, Italy

Abstract. We present a technique which is able to reconstruct severely blended marginals of a simulated set of GAIA-Astrium observations. A satisfactory reconstruction is obtained by using only one free parameter for each marginal.

Key words. Stars: abundances – Stars: photometry – Stars: marginals

1. Introduction

GAIA is the ESA mission to chart a three-dimensional map of the Galaxy. GAIA will provide unprecedented positional and radial velocity measurements with the accuracies needed to produce a stereoscopic and kinematic census of about one billion stars in our Galaxy and throughout the Local Group.

One of the most challenging issues with GAIA is the analysis of crowded fields. Indeed the problem is particulary severe because, in order to perform global astrometry, GAIA will simultaneously observe two distant FoV on the same detector. Moreover, GAIA photometer will not produce direct images but low-dispersion spectra provided by two prisma, one for the red channel (RP, Red Photometer, 640-1050 nm) and one for the blue channel (BP, Blue Photometer, 330-680 nm); these spectra, once acquired, will be sent to the ground not as 2-dimensional images but, except in the case of particularly bright sources ($G < 13$), as marginals projected onto the wavelength axis. Therefore, the most important causes of image blending are: 1) overlapping of spectra of different sources in the same window, 2) overlapping of spectra from two FoVs onto the same focal plane, depending on the scanning law, 3) objects in nearby windows whose spectra extend into the program window, 4) objects for which the on-board detection software has not assigned a window, and 5) barely detectable sources beyond the survey magnitude limit ($20 < G < 22$). In this paper, we address the case of severe image crowding due to the presence of several stellar sources in the same window or in rebuilt mosaics of close windows. At the moment, only stars with a low metal content as observed through the BP channel have been considered, but a more complete study is ongoing.

Send offprint requests to: F. Troisi

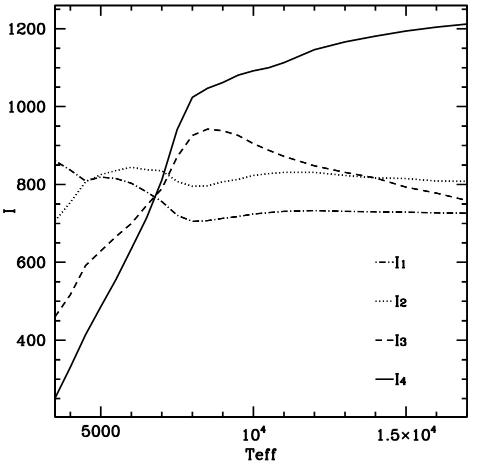

Fig. 1. Height of 4 Moffat curves as derived from the best fit of equation 1 to marginals of different temperature are plotted as a function of T_{eff}. Gravity and metallicity are fixed respectively to Logg=3.00 and [M/H]=-5.00.

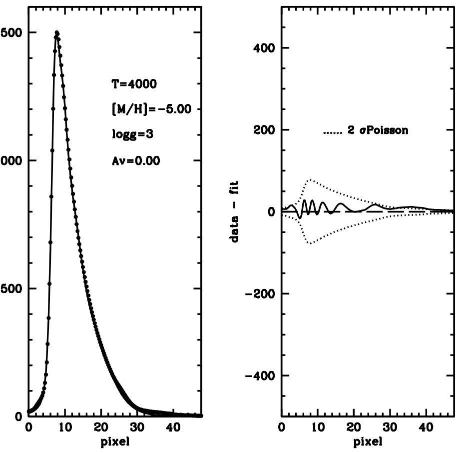

Fig. 2. Left panel: the best fit (continuous line) to the marginal (black dots) of a spectrum with $T_{eff} = 4000K$ and [M/H]=-5.00. The fitting curve has only one free parameter, as described in the text. Right panel: the residuals (continuous line) along with the Poisson noise of the data (dotted line).

2. Our approach

Our study was based on a set of simulated spectra provided by A. G. A. Brown and his group (Brown 2006), for stars of different gravity, metallicity, and temperature values. The spectra were provided at a resolutions four times higher than the real observations and, in order to study the marginals in detail, we used the simulations keeping their full resolution. As a first step we used marginals in the interval $3500 < T_{eff}(K) < 17000$, having fixed Logg=3.00 and [M/H]=-5.00. Following our experience of stellar photometry in crowded fields, we know that the analytical approach is a powerful tool to reconstruct elementary components from severely overlapped images. In fact, deblending overlapped direct images is a classical issue in stellar photometry in crowded fields. Several packages, like ROMAFOT (Buonanno et al. 1988) or DAOPHOT (Stetson 1987) , have been developed in order to deal with the problem of performing fast and precise photometry of large groups of stellar images. However, passing from the case of direct images to that of spectra, we face with the problem of finding a much more flexible analytical function. A few experiments showed that a sum of four elementary Moffat functions (Moffat 1969),

$$I = I_0\left(1 + \frac{(x+x_0)^2}{\sigma^2}\right)^{-\beta} \quad \text{eq (1)}$$

could satisfactorily fulfill the task. The flexibility of equation 1, however, was obtained at the price of keeping 12 free parameters, namely I_{0i}, the height of the curves, x_{0i}, and σ_i, their positions and widths, respectively. Nevertheless, it turns out that the number of free parameters can be easily reduced. In fact, all the parameters are largely monotonic with the temperature and, consequently, a relationship exists among all the parameters of equation 1. Considering that I_4, the height of the fourth Moffat curve, shows the highest gradient with the temperature (see figure 1), we rewrote equation 1 keeping I_4 as the only free parameter and fitted this equation to marginals of different temperatures, obtaining excellent results in all cases. Figure 2 shows (left panel) the best

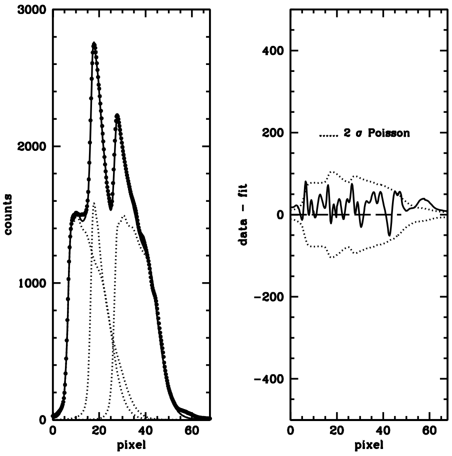

Fig. 3. Left panel: the best fit (continuous line) of three blended marginals, with $T_{eff1} = 8000K$, $T_{eff2} = 4000K$, $T_{eff3} = 8000K$, respectively, and [M/H]=-5.00. The dotted line shows the three best fit for each of the summed spectra. Right panel: the residuals (black line) along with the Poisson noise of the data (dotted line).

fit to the marginal for a simulated spectrum of $T_{eff} = 4000K$. The residuals are shown in the right panel of figure 2, where the Poisson noise of the counts is also shown. Finally we applied the one-parameter curve we have found to the case of blended images, with satisfactory results. Left panel of figure 3 shows the best fit to the marginals of three blended sources, while the residuals are shown in the right panel. We are therefore encouraged to extend our experiments to a large interval of metallicities and to the analysis of the marginals from the red channel.

3. Parallel Developments

While we are extending the analytical approach above described to a larger range of metallicity, at the same time we are testing how effective could be a deblending technique based on a numerical fit in place of the analytical one. The numerical fit is based on a database of simulated marginals across a wide range of physical parameters. In practice, the current adopted procedure consists of a minimization algorithm, based on the comparison among the observed input marginals and the the database ones. This approach is much more straightforward and makes use of the entire morphology of the spectrum in both BP and RP. The first results appear encouraging.

4. Conclusions

This is a preliminary study, which tests a PSF-like approach to the problem of reduction of GAIA blended marginals. The model we developed is simple and requires a very small number of free parameters. This is the first step for the development of an easy, fast and robust software for Gaia data analysis. The next steps we plan to undertake are: 1) extension of the model to a larger temperature interval, 2) extension to higher metallicities and 3) extension to different cases of crowding (contamination by PSF wings, truncated spectra and so on). Further tests are needed in order to study the relationships among the SEDs shapes, temperature and absorption, with the aim to provide decontaminated spectra to the Astrophysical Parameter Coordination Unit 8. In addition, the expected Charge Transfer Inefficiency (CTI) effects has to be considered. CTI is expected to be a severe problem for the astrophysical parameter estimates in general, and in particular for the deblending issue. A deferred charge tail will affect tipically 30 - 50 pixels. This means that the overall SED shape is altered. Thus, future works have to rely on realistic simulations of the astronomical sources as well as of the instrumental properties provided by the GIBIS software tool (Babusiaux et al. 2007).

References

Babusiaux, C. et al, 2007, Gaia Livelink, GAIA-C2-TN-OPM-FC-001-02

Brown, A. G. A., 2006, Gaia Livelink, GAIA-CA-TN-LEI-AB-005-7

Brown, A. G. A., 2006, Gaia Livelink, GAIA-C8-SP-LEI-AB-006

Buonanno, R. 1988, MIDAS Manual, Chapter 5, MIDAS Release 88JAN

Moffat, A. F. J. 1969, A&A, 3, 455

Stetson, P. B. 1987, PASP, 99, 191